Supplementation of αKG along with TGFβ/HIF1α antagonist rescues lung fibrosis in mice with severe SARS-CoV-2 infection.

Garima Joshi[1], Gulistan Parveen[1], Simran Kaur[1], Tejeswara Rao Asuru[1], Naman Kharbanda[1], Anupam Chawla[1], and Tushar K Maiti[1], Prasenjit Guchhait[1]*

[1]Regional Centre for Biotechnology, NCR Biotech Science Cluster, Faridabad, Haryana, India. *Correspondence at prasenjit@rcb.res.in

Supplementary Material:

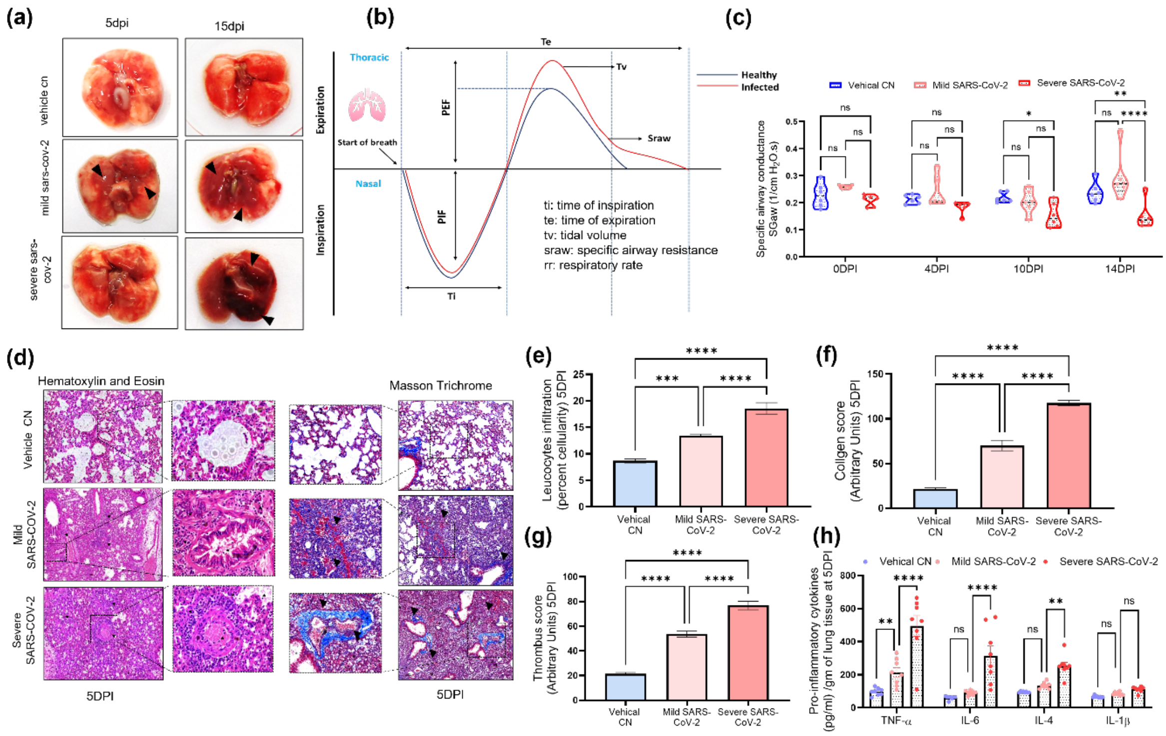

Figure S1 | Extension to main Fig. 1**a,** Representative lung images illustrated a pronounced lung damage in the severe infection group (indicated by black arrows) as compared to mock and mild SARS-CoV-2 infected mice at 5 and 15 DPI. **b,** Schematic representation of the respiratory parameters measured using a dual-chamber plethysmograph, mentioned in main Fig. 1D-F. **c,** Plethysmography measurements at 0, 4, 10, and 14 DPI show significantly reduced specific airway conductance (SGaw) in severe infection. Data are presented as box-and-violin plots. Two-way ANOVA was used for statistical comparisons. **d,** Images of hematoxylin and eosin (H&E) staining (Left panel) and Masson's trichrome (MT) staining (Right panel) of the lung tissue showed persistent inflammation, arrows indicating increased leukocyte infiltration, and thrombus formation, blue staining denoting collagen deposition in the lungs of mice with severe infection as compared to the mild group at 5 DPI. **e-g,** Histology score of tissue leucocyte infiltration, thrombus formation, and collagen deposition of the above Fig. The data are mean ± SEM. One-way ANOVA and Sidak's multiple comparison tests. **h,** The levels of pro-inflammatory cytokines (TNF-α, IL-6, IL-4, and IL-1β) in the lungs were upregulated in the severe infection group as compared to the mild group at 5 DPI. The data are mean ± SEM. Two-way ANOVA with multiple comparisons. For all figures, ns ~ non-significant, *P<0.05, **P<0.01, ***P <0.001 & **** P < 0.0001.

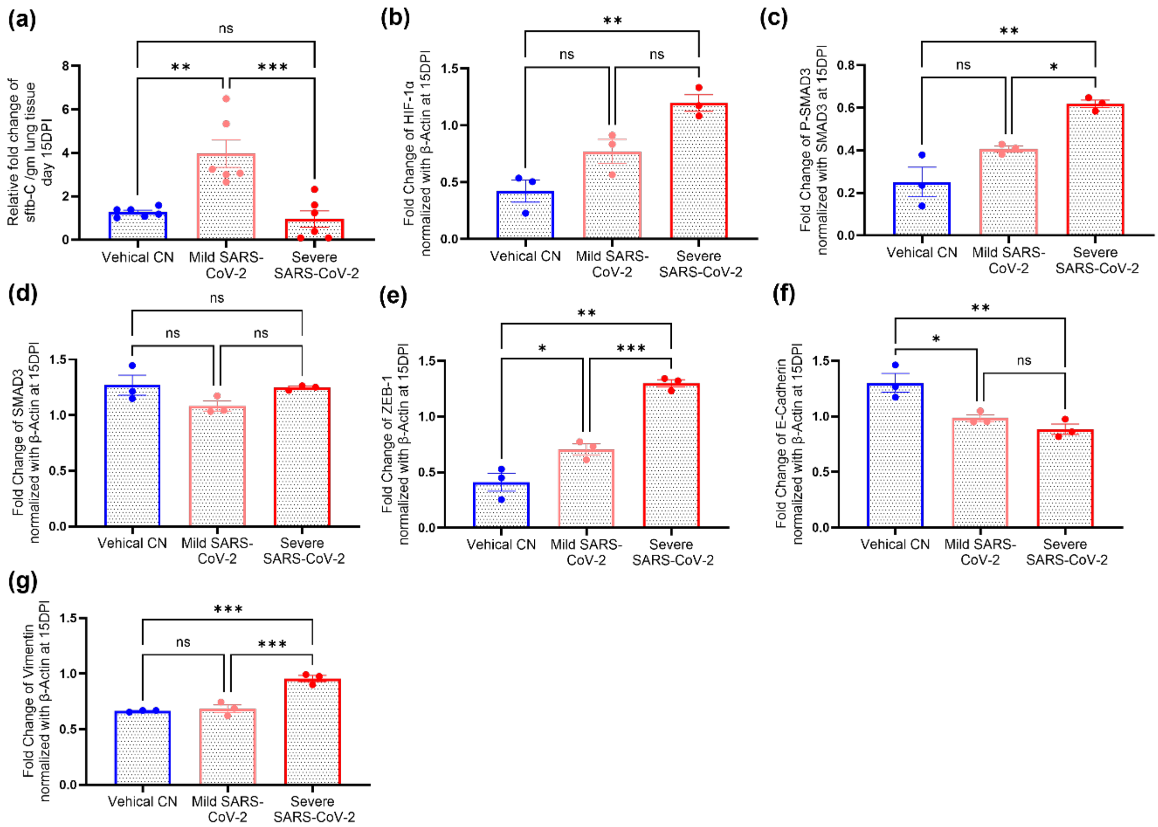

Figure S2 | Extension to main Fig. 2**a,** The level of surfactant protein-C measured from the lung tissue samples, using qRT- PCR at 15 DPI. **b-g,** Densitometric analyses of western blots from three independent animals at 15 DPI, showing expression levels of HIF-1α, SMAD3, P-SMAD3 (normalized to total SMAD3), ZEB1, E-cadherin, and vimentin, with all other proteins normalized to β-actin. Data are presented as mean ± SEM. Statistical significance was determined using one-way ANOVA followed by Sidak's multiple comparison test. ns = non-significant; *P < 0.05; **P < 0.01; ***P < 0.001; ****P < 0.0001.

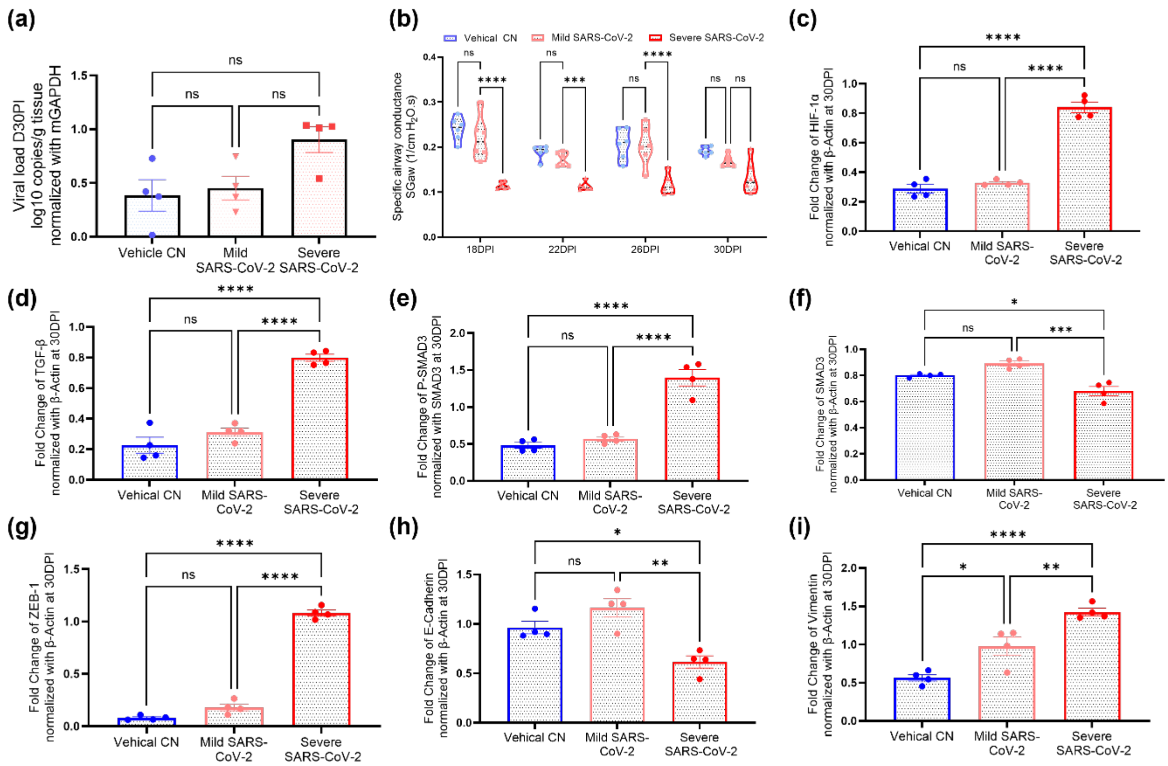

Figure S3 | Extension to main Fig. 3**a,** SARS-CoV-2 viral load in the mice lung was measured using qRT-PCR at 30 DPI **b,** Specific airway conductance (SGaw) was measured using whole-body plethysmography at 18, 22, 26, and 30 DPI. Severely infected mice exhibited a decrease in SGaw as compared to the mild infection group. Data are represented as box-and-violin plots. Two-way ANOVA with multiple comparison tests was used. **c-i,** Densitometric analysis of Western blots from three independent animals at 30 DPI. Expression levels of HIF-1α, TGF-β, SMAD3, ZEB-1, E-cadherin, and vimentin were normalized to β-actin, while P-SMAD3 was normalized to total SMAD3. Data represent mean ± SEM. Statistical analysis was performed using one-way ANOVA followed by Sidak's multiple comparison test. ns = non-significant; *P < 0.05; **P < 0.01; ***P < 0.001; ****P < 0.0001.

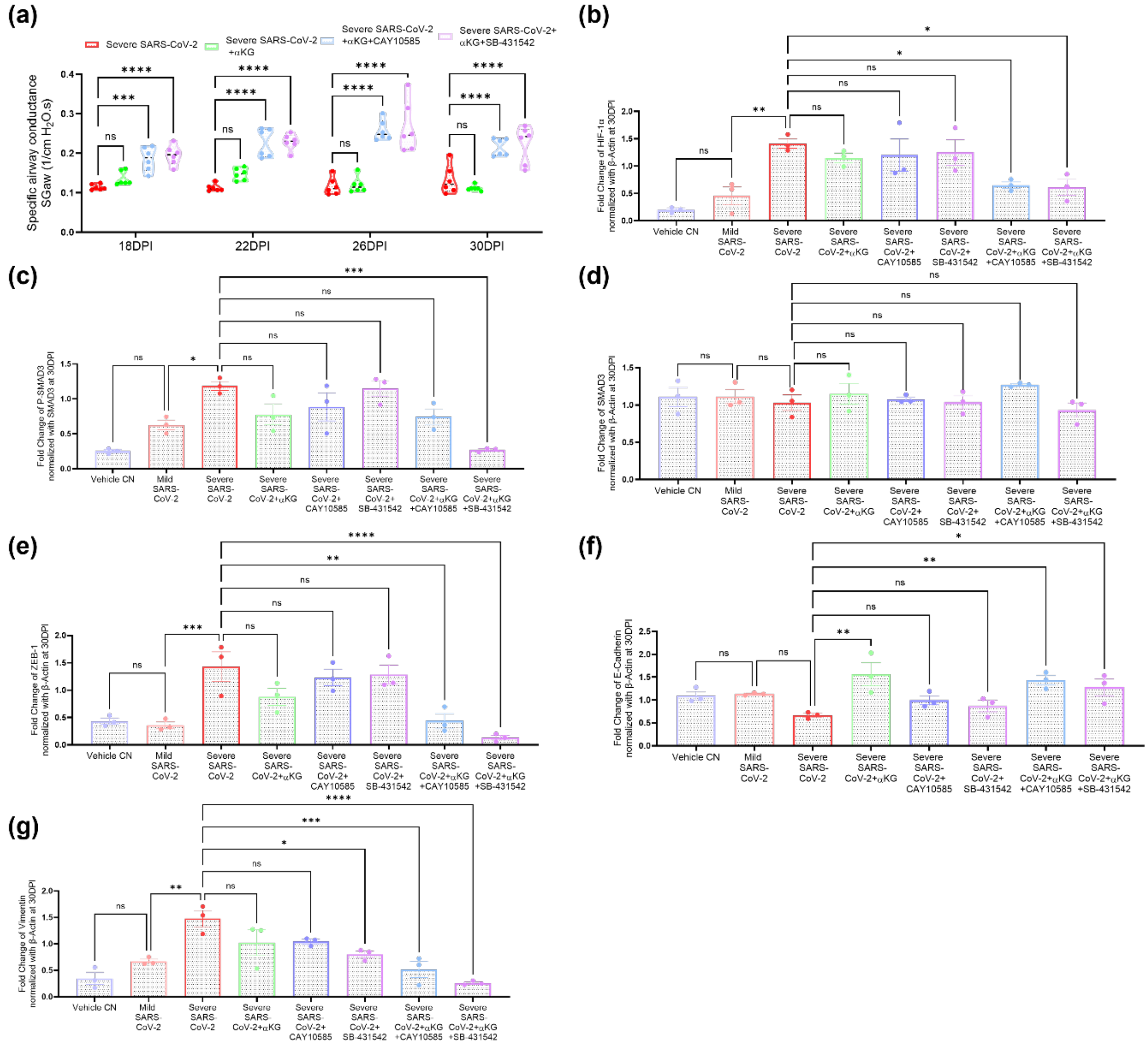

Figure S4 | Extension of Fig. 4 and 5 for 30 DPI: **a,** Specific airway conductance (SGaw) measured using whole-body plethysmography at 18, 22, 26 and 30 DPI. Compared with the severe SARS-CoV-2 infection group, mice treated with αKG along with the antagonist exhibited a significant increase in SGaw. Data are represented as box-and-violin plots. Two-way ANOVA with multiple comparison tests was used. **b-g,** Densitometry of HIF-1α, SMAD3, ZEB-1, E-cadherin, and Vimentin (normalized to β-actin); P-SMAD3 normalized to total SMAD3. Data represent mean ± SEM. One-way ANOVA with Sidak's multiple comparison test was used. ns = non-significant; *P < 0.05; **P < 0.01; ***P < 0.001; ****P < 0.0001.

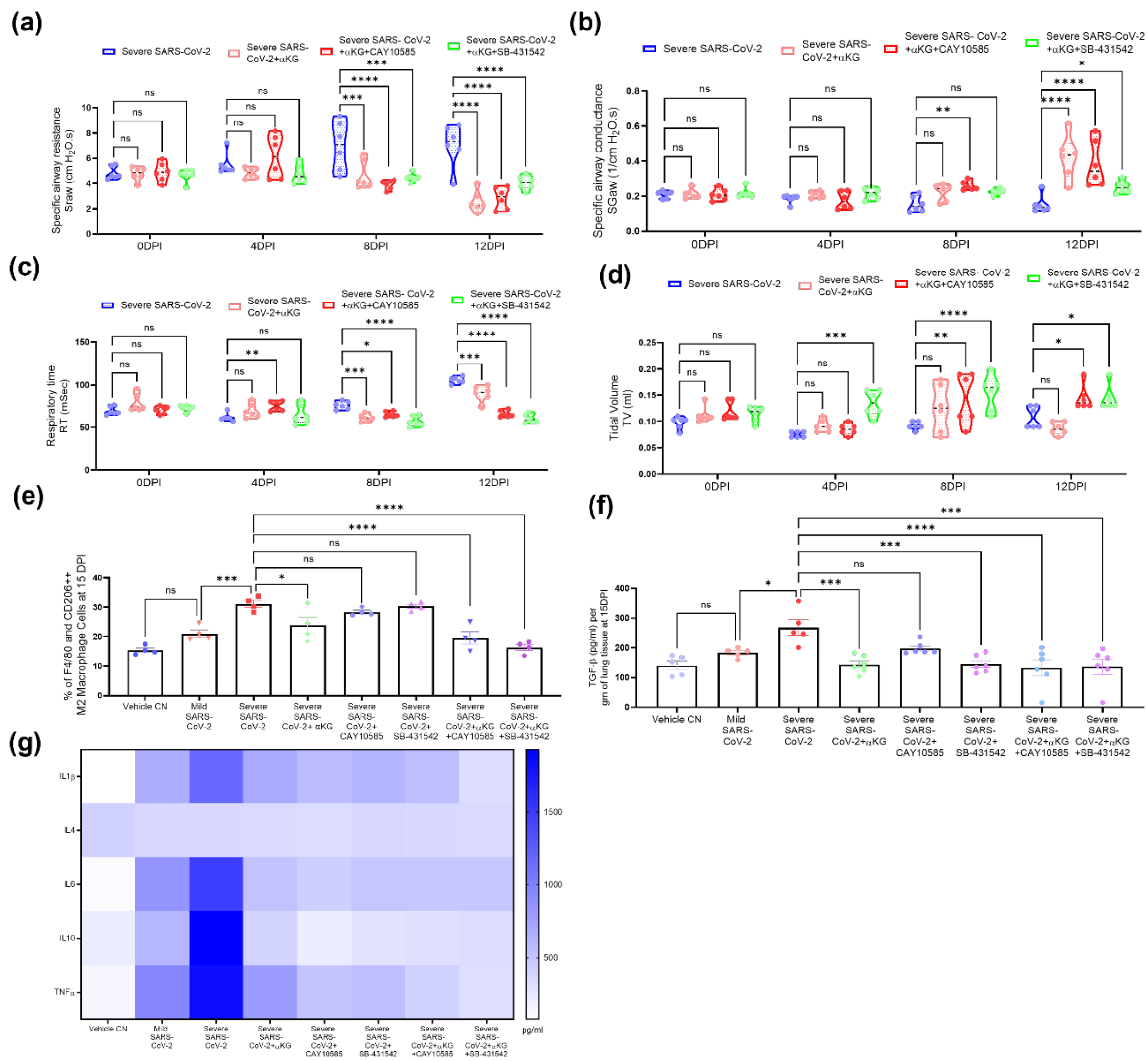

Figure S5 | Extension of Fig. 4 and 5 for 15 DPI. (αKG with TGFβ or HIF1α antagonists at 15 DPI) **a-d,** Plethysmography measurements at 0, 4, 8, and 12 DPI show that αKG treatment combined with HIF1α or TGFβ antagonists significantly reduced the tidal volume (Tv), specific airway resistance (Sraw), and respiratory rate (RR) observed in severe infection. Data are presented as box-and-violin plots. Two-way ANOVA was used for statistical comparisons. **e**, Percentage of CD206++ and F4/80^{++} M2 macrophages was measured using FACS analysis. **(F)** ELISA of lung tissue lysates showed a significant reduction in TGFβ levels following combined treatment. Data represent mean ± SEM. Statistical analysis was performed using one-way ANOVA with Sidak's multiple comparisons. **g,** Cytokine array analysis at 15 DPI reveals reduced pro-inflammatory cytokine levels upon antagonist + αKG treatment, indicating mitigation of the cytokine storm. Data are represented as medians, and a one-way ANOVA was used; Tukey's multiple-comparison test was used. For all graphs ns = non-significant; *P < 0.05; **P < 0.01; ***P < 0.001; ****P <0.0001.

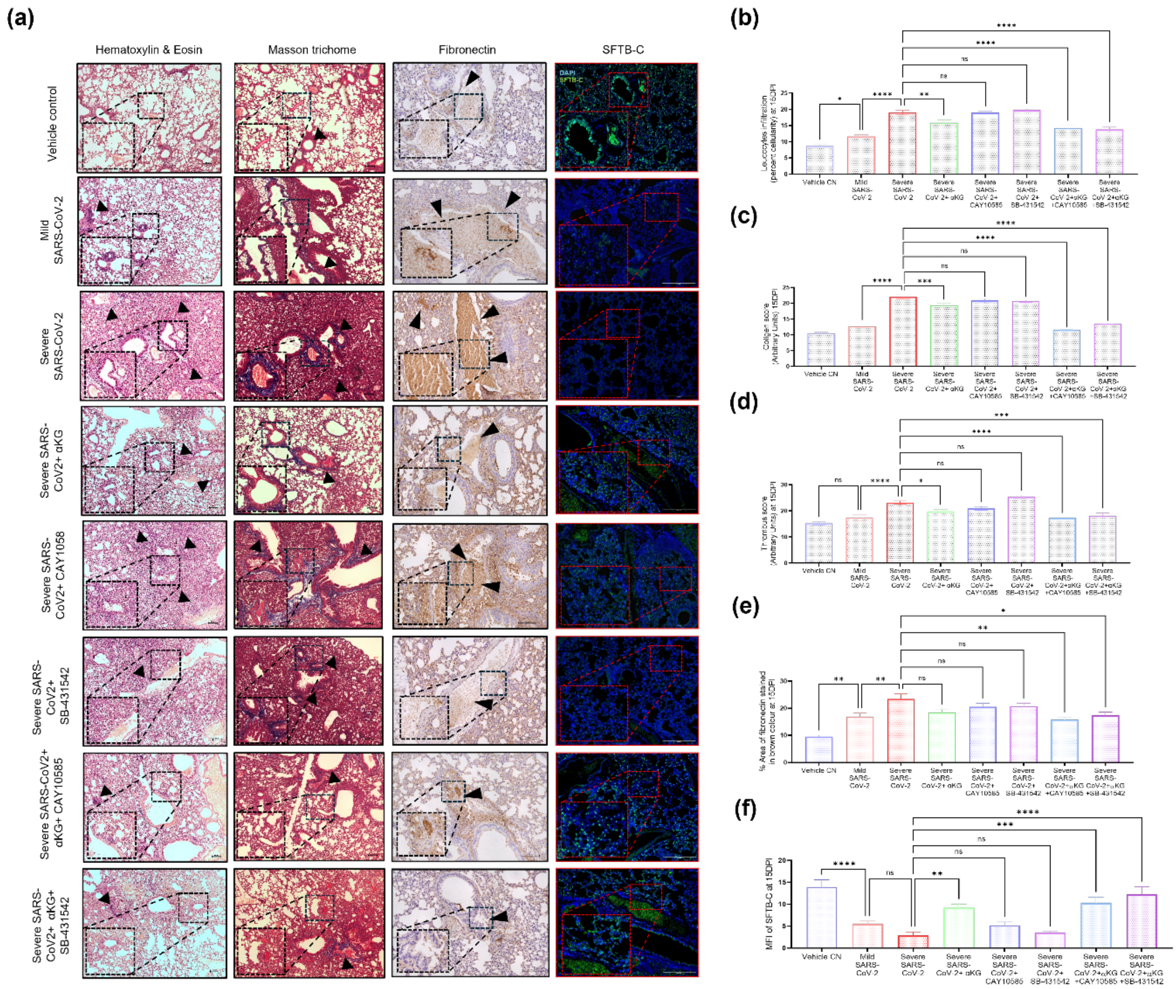

Figure S6 | a, Microscopy images of H&E staining, Masson's trichrome staining, Immunohistochemistry (IHC) for fibronectin, and Immunofluorescence (IF) staining of surfactant protein-C (SFTB-C) of the lung tissue at 15 DPI (~100µm). Arrows indicate immune cell infiltration. **b,** The percentage cellularity score was calculated from 10 different fields of different animals. **c-d,** Quantification of thrombus and collagen scores at 15 DPI. **e-f,** Quantification of fibronectin and Sftb-C at 15 DPI. The data are mean ± SEM. One-way ANOVA and Sidak's multiple comparison tests were used. Statistical significance was assessed using a one-way ANOVA with Sidak's multiple-comparison test. ns = non-significant; *P < 0.05; **P < 0.01; ***P < 0.001; ****P < 0.0001.

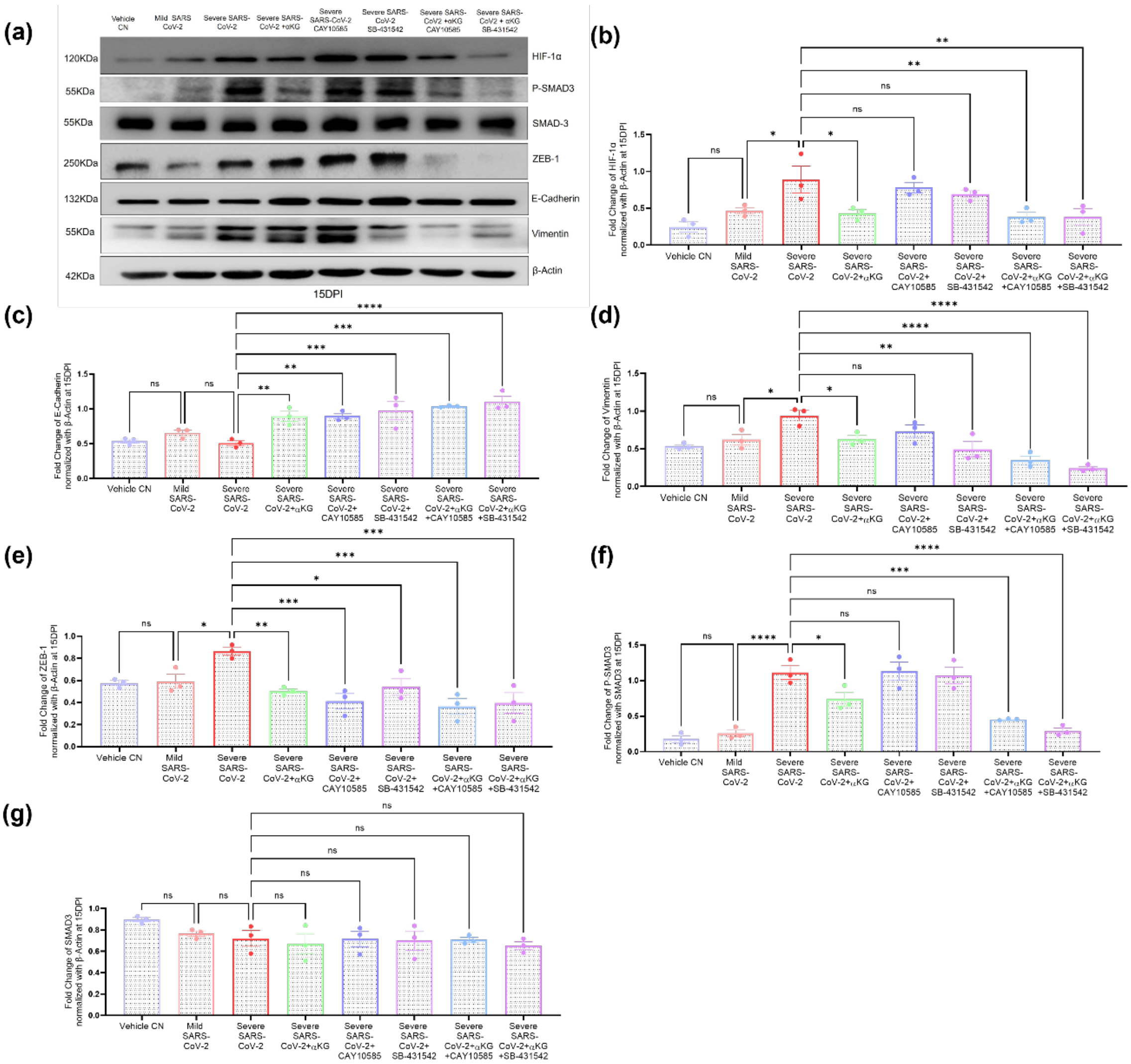

Figure S7 | Extension of Fig. 5 (αKG with TGF-β or HIF-1α antagonists at 15 DPI). **a,** Western blot analysis of EMT-associated proteins (HIF-1α, P-SMAD3, SMAD3, ZEB-1, E-cadherin, Vimentin) demonstrates pronounced inhibition with αKG alone and further enhancement with antagonist combinations. **b-g,** Densitometry of HIF-1α, SMAD3, ZEB-1, E-cadherin, and Vimentin (normalized to β-actin); P-SMAD3 normalized to total SMAD3. Data represent mean ± SEM. One-way ANOVA with Sidak's multiple comparison test was used. ns = non-significant; *P < 0.05; **P < 0.01; ***P < 0.001; ****P < 0.0001.

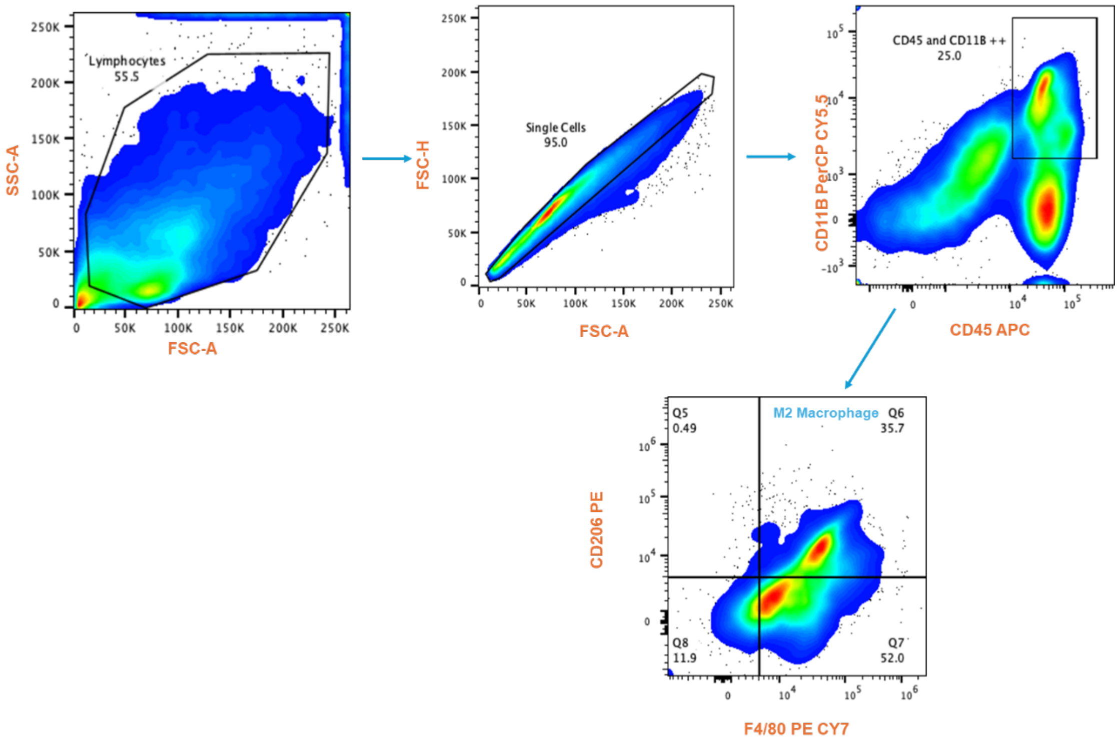

Figure S8 | Showing the gating strategy for M2 macrophage from the mice lung single cell suspension.

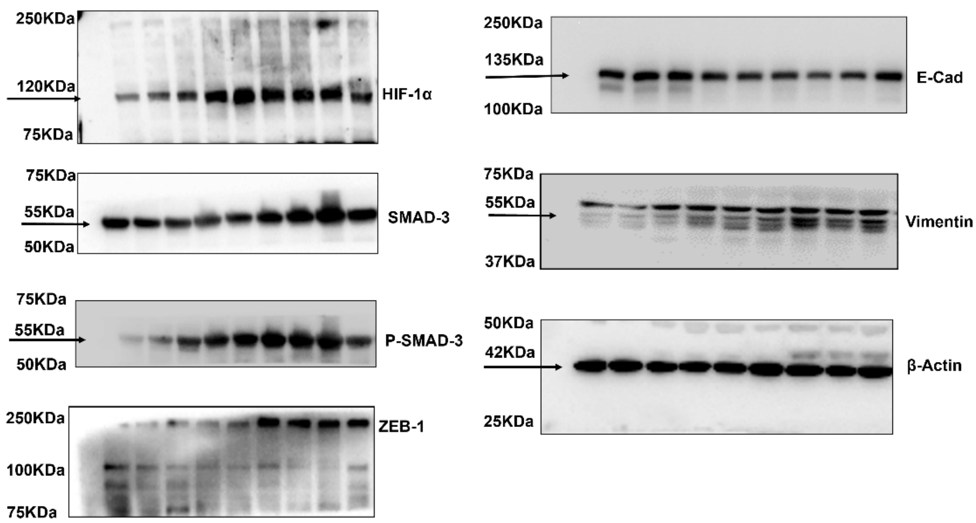

Figure S9 | Raw data for the western blot main figure 2h.

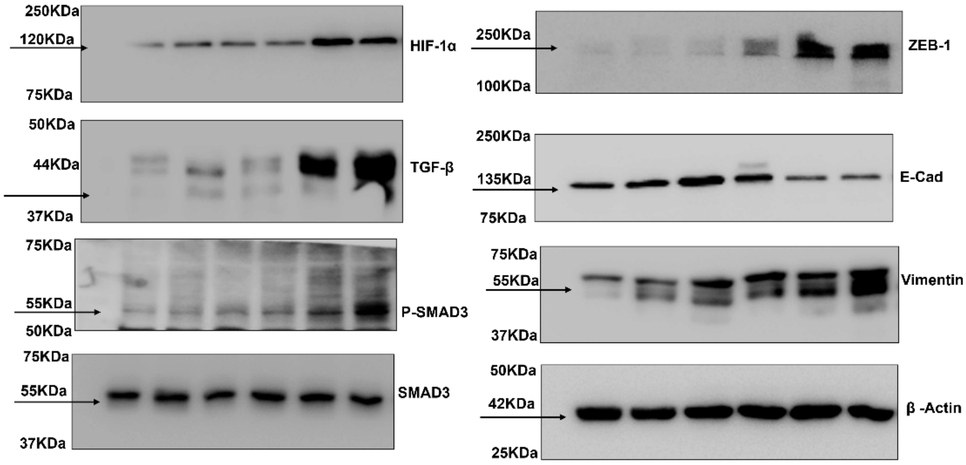

Figure S10 | Raw data for the western blot main figure 3k.

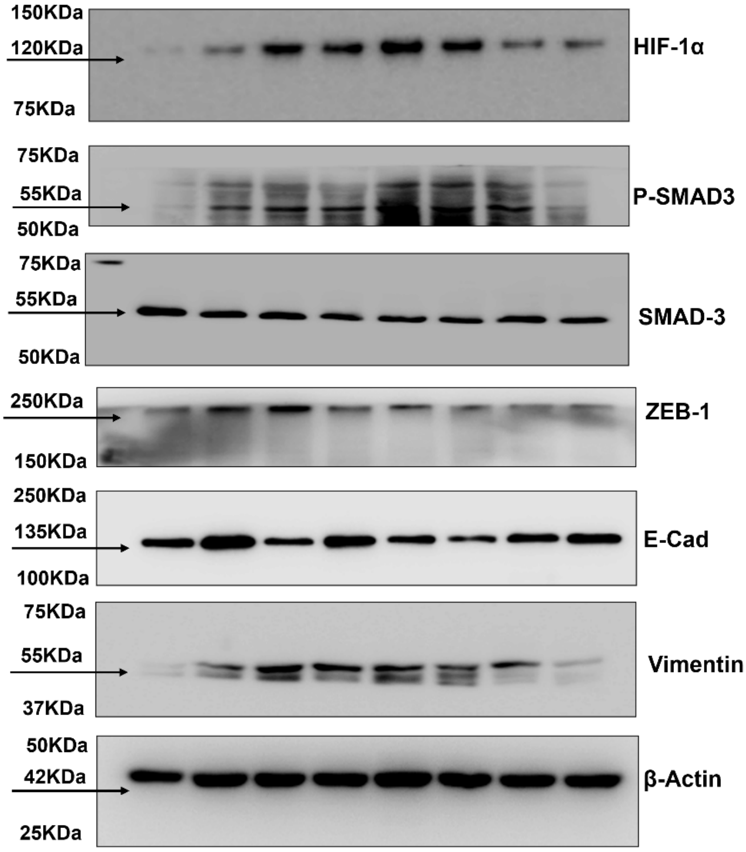

Figure S11 | Raw data for the western blot main figure 5h.

Table S1 | Details of viral strains

Virus Strain	Source	Identifier
SARS-CoV-2	BEI	USA-WA1/2020
Ad5-hACE2	Viral Vector Core (University of Iowa, Iowa, USA)	VVC-McCray-7723

Table S2 | Primer List

Gene	Forward primer (5'-3')	Reverse primer (5'-3')
mGAPDH	ACCACAGTCCATGCCATCAC	TCCACCACCCTGTTGCTGTA
Spike	GTGTCATGGTGGCGAATAAG	TCGTTGAACCAGGGACAAGG
mSFTB-C	GTAGCAAAGAGGTCCTGATG	CCTACAATCACCACGACAA

Table S3 | Antibody List

S. No.	Antibody	Manufacture	Clone	Catalog No.
1	β- ACTIN	Cell Signalling Technology	1.30E+06	4970S
2	ACE-2	Cell Signalling Technology	E506J	92485T
3	HIF-1α,	Cell Signalling Technology	D2U3T	14179S
4	P-SMAD3	ABclonal	AP0727	ARC0170
5	SMAD3	Abcam	EP568Y	Ab40854
6	TGF-β	Cell Signalling Technology	E5M6F	41896 S
7	ZEB-1	Cell Signalling Technology	D80D3	3396
8	E-Cadherin	Cell Signalling Technology	2.40E+11	3195
9	Vimentin	Cell Signalling Technology	D21H3	5741
10	DAPI	Cell Signalling Technology	-	4083S
11	Hoechst	Invitrogen		33342
12	Fibronectin	ABclonal	ARC2692	A12977
13	Surfactant-Protein-C	AbCam	EPR19839	AB211326
14	CD45	BioLegend	104	109814
15	CD11b	BioLegend	M1/70	553310
16	F4/80	BioLegend	BM8	123110
17	CD206	BioLegend	MR5D3	565250
18	Goat anti-rabbit HRP conjugated	Cell Signalling Technology	-	7074
19	Goat anti-mouse HRP conjugated	Cell Signalling Technology	-	7076
20	Goat anti-rabbit AF488	Invitrogen by Thermo Scientific	-	A11008
21	Goat anti-rabbit AF594	Invitrogen by Thermo Scientific	-	A11037
22	Goat anti-mouse	Invitrogen	-	A-11029

Table S4 | Consumables and reagents

S. No.	Regents/Kit	Manufacture	Catalog No.
1	TGF-beta 1	AbCam	Ab50036
2	CAY10585	CAYMAN chemicals	10012682
3	SB-431542	Targetmol	T1726
4	Liberase	Sigma	5401127001
5	DNAase	Sigma	10104159001
6	Vetbond Tissue Adhesive	3M	1469SB
7	Dulbecco's modified Eagle's medium (DMEM)	Invitrogen, USA	12800-017
8	Roswell Park Memorial Institute (RPMI 1640)	Sigma Aldrich, USA	R4130-1L
9	Fetal bovine serum (FBS)	Gibco Invitrogen, USA	10270-106
10	Penicillin/Steptomycin	Sigma Aldrich, USA	P4333
11	RNAiso Plus	Takara Bio,Japan	9109
12	iScript cDNA synthesis kit	BIORAD Laboratories USA	1708891
13	Nuclease-free water	Promega,USA	P1193
14	SYBR GREEN Supermix	BIORAD Laboratories USA	1725124
15	RIPA lysis buffer	Sigma Aldrich, USA	R0274
16	Protease-phosphate inhibitor	Thermo Scientific Life Tech, USA	78441
17	Bovine serum albumin (BSA)	BioString, USA	BS100053-500
18	Mouse TGF-β ELISA	Finetest	EH0287
19	TNF-α	BD Biosciences	558299
20	IL-6	BD Biosciences	562236
21	IL-10	BD Biosciences	558300
22	IL-1β	BD Biosciences	560232
23	IL-4	BD Biosciences	558298

Table S5 |Software and Algorithms

S. No.	Software and Algorithms
1	GraphPad prism v10 (GraphPad Software)
2	EMKA iox2 (TECHNOLOGIES iox software v.2.11.1)
3	Image J (Fiji)
4	FlowJo (FlowJo LLC, Oregon)
5	CurveExpert
6	Alpha imager
7	LAS X office
8	Biorender
10	Sciex OS platform (v3.1.6.44, Sciex, MA, USA)
11	Perseus (v 2.0.7.0)
12	ShinyGO (v 0.82)
13	RStudio (v 4.4.1)
14	SRplot